N. Bence[1], A.I. Lengyel[2], Z.Z. Tarics[2]

[1]Uzhhorod National University, 88000, Uzhhorod, 14, Universitetska Str., Ukraine
[2]Institute of Electron Physics, NAS of Ukraine, 88000, Uzhhorod, 21, Universitetska Str., Ukraine,
e-mail: bencenorbert007@gmail.com

POMERON MODELS AT LHC ENERGIES

Purpose. The existing experimental data on the elastic scattering of protons (antiprotons) by protons, including those obtained at the Collider, are not in doubt for non-exponential behavior of differential cross-section. Our task is to choose the most adequate analytical model that describes this behavior of the differential cross sections for elastic pp- and $\bar{p}p$ scattering.
Methods. Pomeron alternatives for describing the non-exponential behavior of the diffraction cone in differential pp- and $\bar{p}p$ elastic cross-section are investigated.
Results. It was shown that the pomeron amplitude with two tewrms with different t-dependences is strongly suggested by the data.
Conclusions. The values of the slope $B(s,t)$ and curvature parameter $C(s,t)$ have been calculated for different Pomeron model within the wide s – and low t – range with the allowance made for the diffraction cone shape. The absolute values of the curvature parameter $C(s,0)$ is predicted to be decreasing depending on s and change of sign at asymptotically large energies.
Keywords: elastic scattering, high energy, pomeron, slope, curvature.

Introduction

Elastic scattering at high energy and low momentum transfer is crucial to the choice of appropriate pomeron model to description the data of experiment. In this connection the knowledge of such fundamental physical values of the elastic scattering as the total $\sigma_{tot}(s,t)$, differential cross sections $d\sigma(s,t)/dt$, slope $B(s,t)$ and curvature parameter $C(s,t)$ (for brevity, simply as curvature) is decisive in checking up the certain strong interaction model.

Recently the revealing the novel and unexpected non-exponential behavior of the elastic proton-proton differential cross-section at LHC energies [1, 2] have initiated the revision of the methods of investigation [3–5]. The total cross sections measured at LHC energies [2, 6] indicates that the «asymptopia» (i.e. the Froissart boundary) is attained.

Taking into account that at high energies the values of $\sigma_{tot}(s,t)$, $B(s,t)$ and $C(s,t)$ were determined in the same LHC experiments and keeping in mind mentioned above, the development of the up to date criteria of the unified approach for their determination seems to be natural.

It has been shown in [7, 8] that, starting with the available experimental data, we are up against a considerable precise data for the determination of the above mentioned parameters.

A modified method of determination of the slope, curvature and phase on the basis of the experimental data has been suggested in [9]. A critical analysis of the data $\sqrt{s} = 19.4$, 546 and 1800 GeV has been performed allowing one to find both the slope and the curvature usually defined as

$$B(s,t) = \frac{d}{dt} \ln\left(\frac{d\sigma(s,t)}{dt}\right), \qquad (1)$$

$$C(s,t) = \frac{1}{2}\frac{dB(s,t)}{dt}. \qquad (2)$$

It should be noted that despite the small effect the curvature affects the small-t diffraction scattering values, thus it should be taken

into account in the elastic scattering analysis [10]. Similarly, we have also used the procedure of overlapping t-bins [7,10] to reconstructing the local nuclear slopes from the experimental angular distributions as well as the curvature $C(s,t)$ at $t = 0$ when the $\sqrt{s}$ reaches the Tevatron energies. It was applied the physical threshold properties of the scattering amplitude expressed in the nonlinear Pomeron trajectory [11]:

$$\alpha(t) = 1 + \alpha't + \gamma(\sqrt{t_0} - \sqrt{t_0 - t}), \quad (3)$$

where $t_0 = 4m_\pi^2$ the lowest threshold, m_π - pion mass. Concerning the search for asymptopia Block and Chan [12] considered the curvature $C(s,0)$ as a sensitive indicator of the transition to asymptopia going from positive values at the ISR energies, to be zero at the Tevatron energy. They have expected for any model, which approaches the sharp black disc limit that the curvature at $t = 0$ should become negative at high energies. In this relation the idea arises to revise available elastic pp- and $\bar{p}p$-scattering data for high energies within a wide interval of s and low $|t|$ starting from the method suggested in [9]. Due to the unified approach in calculating the characteristics B and C we shall predict their energy behavior. The similar procedure has been executed earlier for the energies ranging up to the Tevatron energies (~ 2 TeV) in the approximation of the unified origin of the leading singularity for the pp- and $\bar{p}p$-scattering [7]. It has been shown that the curvature for the pp- and $\bar{p}p$ -scattering shows different behavior over the energy region under study. Later the change of sign for curvature $C(s,t = 0)$ when $\sqrt{s}$ exceeds the Tevatron energy was predicted in model with two-components Pomeron and Odderon model [10]. It makes sense to recall the remarks on the asymptopia which was correctly noted in [13] long time ago: «for the moment, the situation is such that we do not find any evidence for new and not old-fashioned physics in hadronic diffraction at high energies. Odderon and threshold effects may be there, but do not seem to be relevant for the description of the bulk of the interactions: total cross-section, ratio rho, differential cross section, etc.» The time has come when you can reconsider these predictions. Now the ideal place to search for

the asymptopia is the LHC. In [14] among others the investigation of the forward slope $B(s)$ and interaction radius connected with impact parameter b for nucleus has been done. The authors have come to the conclusion that we «are still extremely far from the asymptopia, the region where some known asymptotic relations should hold». There we shall study the s- and t-behavior of B and C within the framework of the phenomenological model which considers naturally the curvature as the manifestation of a complex structure of the Pomeron in the first cone region and at all available energies up to $\sqrt{s}$ =13 TeV and, thus, recalculate the $B(s,t)$ and $C(s,0)$ values. Our strategy for the investigation of the shape of a non exponential behavior of the diffraction cone and it consequences will be the following:

1) First we have collect the data set of differential cross section for pp- and $\bar{p}p$-scattering where the non-exponential behavior of diffraction cone is clearly present in broad area of energy and appropriate interval of momentum transfer to select the most suitable form of this non-exponentiality.

2) Next we chose the best form of Pomeron for description of selected data set, combining the nonlinear Pomeron trajectory and non-exponential residue contribution.

Data selection

To look for non-exponential behavior similar to that observed in the CERN [1, 2] we have separate those experimental data for pp- and $\bar{p}p$-scattering which contains the number of experimental points $n \cong 100$, namely: E_{cm} = 19.4 [15]; 23.5; 30.7; 44.7; 52.8; 62.5 GeV [16]; 8 [1] and 13 TeV [2] for pp-scattering and E_{cm} = 546 GeV [17] for $\bar{p}p$ -scattering. To determine the interval of momentum transfer for the experimental data, where it is necessary to carry out the investigations, we shall use the overlapping bin procedure (OBP) [7,10] whose idea is as follows. The whole interval over the momentum transfer $|t|$ is divided into bins with a reasonable number of experimental data point (≈ 10) so that within the range of the bin the given experimental points can be approximated by the

$$\left(\frac{d\sigma(t)}{dt}\right)_i = \left|a_i e^{b_i t}\right|^2, \qquad (4)$$

a_i and b_i are free parameters. Wherein the bins are shifted with respect to each other by one or more measuring channel in such a manner that they overlap so that for each investigated energy we have obtained the set of «experimental» value of local slopes b_i (see Fig. 1) close to the original number of true experimental points of $d\sigma/dt$. The error bars Δb_i shown in the figure represent the fitting uncertainty. In the area of interest we observe the following features of the structure of the slope (Fig. 2):

- sharp growth of the local slopes, when approaching the region of interference the Coulomb and nuclear amplitudes ($|t| < 0.01 GeV^2$);

- slowly decreasing sequence of local values distributed along a smooth curve with oscillation around it;

- collapse of the slope at $|t| < 1 GeV^2$ corresponding to the dip in the $|t|$.

Having carried out such a procedure for all separate energy of selected data sets of the differential cross sections pp- and $\bar{p}p$ scattering, we have to implement two cutoffs: first, one needs to be away from the Coulomb interference region and second to be far from region, where rescatterings are important, $t_c < |t| < t_d (GeV^2)$ where t_c and t_d are the correspond limit values (see Tab. 1). The remaining data is the comprising rather large number of experimental points in order to determine the t-dependence of the slope and curvature. It is convenient to take it with the help of the «experimental» points of the slopes obtained by OPB as the deepest point of the local bins set. This criterion of the diffraction cone end corresponds to the common concept of the «first diffraction cone».

Choice of curvature shape

There we shall study the s- and t-behavior of slope B and curvature C within the framework of the phenomenological model which considers naturally the curvature as the revelation of the threshold behavior of the scattering amplitude in the t-channel and the shape of proton in the first cone region, thus, recalculate the $B(s,0)$ and $C(s,0)$ values. Here we shall divert the reader's attention from our attempt to account for the oscillations observed in the slope and confine ourselves to the consideration only the smooth component of the diffraction cone fine structure, i.e., the curvature. To do this, we will choose two possible non exponential behavior of the differential cross section within the diffraction cone at fixed energy [7]:

$$\frac{d\sigma(t)}{dt} = a e^{\delta t + \gamma \sqrt{t_0 - t}}, \qquad (5)$$

or [1]

$$\frac{d\sigma(t)}{dt}) = a e^{bt + ct^2}. \qquad (6)$$

To visualize the quality of the fit of $d\sigma(t)/dt$ and the choice of a better approximation of non-linearity, we shall use two methods: the OBP and the normalized differential cross sections $R(t)$. In the first case each bin contains 8 experimental points. The overlap of bins is maximal, i.e. each bin shifts to one experimental point relative to the neighboring one (see Fig. 1). For the second the normalized experimental data:

$$R_{exp}(t) = \frac{(d\sigma/dt)_{exp} - (d\sigma/dt)_{lin}}{(d\sigma/dt)_{lin}}, \qquad (7)$$

where $(d\sigma/dt)_{exp}$ – experimental points, $(d\sigma/dt)_{lin}$ – the approximation of all experimental points at given fixed energy from the selected interval of momentum transfer by a linear exponential (4). Accordingly, the theoretical values $R_{th}(t)$ are calculated for (5) and (6) with the parameters of the best fit to the experimental data for each individual of 9 sets.

$$R_{th}(t) = \frac{(d\sigma/dt)_{th} - (d\sigma/dt)_{lin}}{(d\sigma/dt)_{lin}}, \qquad (8)$$
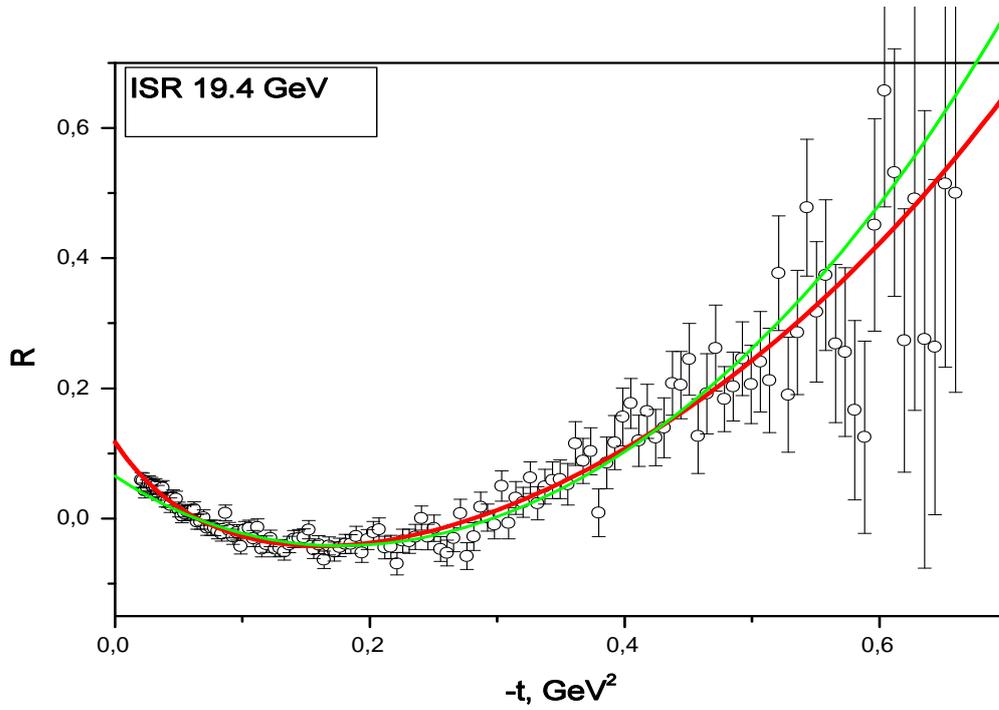
Figure 1: The experimental function $R_{exp}(t)$, calculated by (7) for energy $\sqrt{s}$ = 19.4 GeV.Solid red line - calculated function $R_{th}(t)$ by the formula (8) for fitted parameters by (5). Solid green line - calculated function Rth(t) by (8) for fitted parameters by (6), bar - fitting uncertainty.
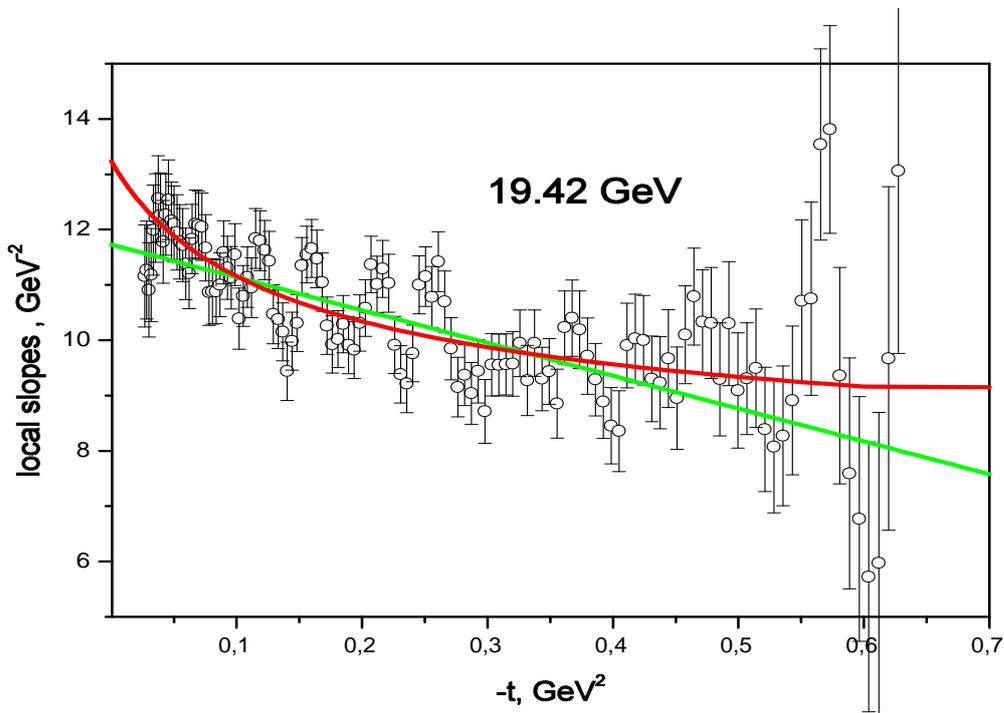

Figure 2: The local slopes bi, calculated wit help the procedure OBP by (4), bar - fitting uncertainty. Solid red line - calculated by the formula (9) for fitted parameters by (6). Solid green line - calculated by the formula (9) for fitted parameters by (6), bar - fitting uncertainty.

Table 1: Compilation of data. t_c – lover and t_d – upper limit values of the t-range; n – number of experimental points; a and b – linear fit parameters. Set No 1-6 and 8-9 – pp-scattering, set No 7 – $\bar{p}p$ - scattering.

Set	E_{cm}, GeV	$|t_c|, GeV^2$	$|t_d|, GeV^2$	n	$a, mb/GeV^2$	b, GeV^{-2}
1	19,42	0.0206	0.6599	134	72.60	10.60
2	23.5	0.042	0.53	65	66.54	10.31
3	30.7	0.038	0.70	102	72.06	10.32
4	44.7	0.05375	0.28875	99	79.22	11.49
5	52.8	0.0308	0.396	111	85.67	11.72
6	62.5	0.0215	0.49	53	92.7	12.49
7	546	0.0325	0.3175	58	196.2	14.76
8	8000	0.0285	0.19478	30	527	19.39
9	13000	0.0207	0.166	86	633.4	20.43

From the comparison of the results of the fit for the two models (5) and (6), we see that it is difficult to give preference to one or another approximation by the function R(t). Instead, such a comparison of the results of the calculation of the slopes should definitely favor the approximation (5) as it clearly seen from Fig. 2. The same pattern is observed for all other cases from the selected ones. The general behavior of the curvature with increasing energy in both cases is the same. As it was mentioned in [9] the curvature is significantly stronger than that found using the simple quadratic-exponential (c=const) fits which have been traditional for analizing experiments [1, 2]. Therefore alternatively, as a non-linear rexponential factor, we will use the approximation (5).

Choice of the Pomeron

The next step is to choose the Pomeron contribution to the scattering amplitude, which corresponds to the observed behavior (decreasing) of the curvature $C(s,0)$. Taking into account the analysis performed above, we will choose a common form of the Pomeron contribution to the cross-symmetric scattering amplitude as

$$A_i(s,t) = g_i \tilde{s}^{\alpha_p(t)} e^{\varphi(t)}, \qquad (9)$$

where

$$\tilde{s} = -i\frac{s}{s_0}, s_0 = 1\text{GeV}^2, \qquad (10)$$

$\alpha_p(t)$ – non-linear Pomeron trajectory (3). Non-linear exponential residue function is [8, 10].

$$\varphi(t) = bt + \beta\sqrt{4m_\pi^2 - t} - 2m_\pi. \qquad (11)$$

The differential cross section for each i-set has the form

$$\left(\frac{d\sigma(t)}{dt}\right)_i = \frac{\pi}{s^2}|A_i(s,t)|^2. \qquad (12)$$

i – number of set (1...9) at fixed energy ($\sqrt{s} = $ 19,4; 23,5; 30.7; 44.7; 52.7; 62.5; 546; 8000; 13000 GeV). Next, we will perform an overall (Pomeron) fit of all the above selected 9 sets of data by (9)-(14) with (3) where g_i - the normalization factor for each set separately. Consider three variants of the combination of the contribution of the non-linear exponential behavior of $\varphi(t)$ and the nonlinear trajectory of the Pomeron $\alpha_P(t)$ [7, 8]:

$$\beta \neq 0, \gamma \neq 0, \cdots (I)$$

$$\beta \neq 0, \gamma = 0, \cdots (II)$$

$$\beta = 0, \gamma \neq 0, \cdots (III)$$

The curvature $C(s,t)$ for variants I-III respectively hase the form

$$C(s,t) = -\frac{1}{2}\frac{\gamma\ln\frac{s}{s_0} + \beta}{(t_0 - t)^{3/2}}, \qquad (13)$$

$$C(s,t) = -\frac{1}{2}\frac{\beta}{(t_0 - t)^{3/2}}, \qquad (14)$$

$$C(s,t) = -\frac{1}{2}\frac{\gamma\ln\frac{s}{s_0}}{(t_0 - t)^{3/2}}, \qquad (15)$$

Table 2: The parameters of the Pomeron fit for I-III variants

	I		II		III	
Parameter	Value	Error	Value	Error	Value	Error
g_1	64.48	0.18	63.52	0.16	58.87	0.11
g_2	64.40	0.34	62.53	0.33	58.14	0.29
g_3	72.41	0.22	71.67	0.21	68.18	0.19
g_4	73.50	0.23	73.01	0.22	68.15	0.17
g_5	78.27	0.18	77.50	0.17	73.27	0.13
g_6	81.38	0.17	80.76	0.16	77.01	0.13
g_7	180.5	0.8	180.7	0.8	177.7	0.7
g_8	450.7	0.7	457.1	0.5	463.2	0.6
g_9	526.0	0.8	534.8	0.5	544.5	0.7
b_p	0.8383	0.0494	1.414	0.018	3.019	0.005
α'	0.4144	0.045	0.3518	0.007	0.2308	0.0029
γ	0.05411	0.00511	–	–	-0.1153	0.0002
β	-2.149	0.048	1.619	0.023	–	–
χ^2/dof	2.98		3.20		5.77	

As can be seen from Table 2. fit by the variant I with non-linear trajectory and a non-linear exponential residue function is well consistent with experiment data. This makes us choose the variant I for the Pomeron contribution to the scattering amplitude. In this case the relative nonlinear trajectory plays the minor role, and option III is by no means acceptable [3]. The behavior of $C(s, 0)$ in this case, calculated by (13), has a decreasing character.

Conclusions

We have studied the phenomenology of the pp- and $\bar{p}p$ - elastic scattering within a wide energy range from tens of GeV to tens of TeV by using a model in which the analytical properties of the scattering amplitude are accounted for by the threshold singularity in the cross-channel. It has been shown that such features reflect adequately the smooth part of the t-dependence of the slope in a form of a concave curve found with the help of the model-independent procedure of overlapping t-bins. The calculated values of the curvature differs from zero due to that we have chosen the physical threshold in the cross channel as $t_0 = 4m_\pi^2$ and non-exponerntial residue of pomeron pole. To clarify the question whether the non-linear exponential behavior of the diffraction cone is due to a nonlinear trajectory or non-linear exponential residue function it is necessary additionally take into account the novel LHC data. We emphasize that the non-exponential function $\varphi(t)$ entering to in the Pomeron pole residue, as well as the non-linearity of its trajectory $\alpha_p(t)$ is strongly suggested by the data. As a result, one can observe that the curvature $C(s, 0)$ has a tendency to decrease and change the sign. It has been shown that $C(s, 0)$ calculated with the inclusion of the non-linear exponential residue function together with the non-linear Pomeron trajectory decreases going into the «asymptopia» mode. As for the energy dependence of the curvature, $C(s, 0)$ calculated with the inclusion of above mentioned residue function together with the non-linear Pomeron trajectory decreases, as expected, crossing the energy axis at $\sqrt{s} > 10^4$ TeV.

REFERENCES

[1] Antchev, G., Aspell, I. *et al.* (TOTEM Collaboration) (2015), «Evidence of non-exponential elastic proton-proton differential cross-section at low $|t|$ and $\sqrt{s} = 8$ TeV by TOTEM», Nucl. Phys. B, V. 899, pp. 527–546.

[2] Antchev, G., Aspell, I. *et al.* (TOTEM Collaboration)(2017), «First determination of the ρ parameter at $\sqrt{s} = 13$ TeV – probing the existence of a colorless three-gluon bound state», Eur. Phys. J. C, V. 79, pp. 785 (1–26).

[3] Jenkovszky, L., Lengyel, A. (2015), «Low-$|t|$ structures in elastic scattering at the LHC», Acta Phys.Pol. B, V. 46, pp. 863–877.

[4] Khose, V.A., Martin, A.D. and Ryskin, M.G. (2018), «Elastic proton-proton scattering at 13 TeV», Phys. Rev. D, V. 97, pp. 034019(1–6).

[5] Martynov, E. and Nicolescu, B. (2018), «Did TOTEM experiment discover the Odderon?», Phys. Lett. B, V. 778, pp. 414–418.

[6] Antchev, G., Aspell, I. *et al.*(TOTEM Collaboration) (2016), «Measurement of Elastic pp Scattering at $\sqrt{s} = 8$ TeV in the Coulomb-Nuclear Interference Region - Determination of the ρ Parameter and the Total Cross-Section», Eur. Phys. J. C, V. 76, pp. 661 (1–21).

[7] Desgrolard, P., Lengyel, A.I. and Martinov, E.S. (1997), «Nonlinearities and Pomeron non-factorizability in convention diffraction», Nuovo Cimento, V. 110, pp. 251–266.

[8] Bence, N., Lengyel, A.I., Tarics, Z.Z. (2019), « Comparative analysis of analytical models for high energy pp-scattering», IEP-2019. International Conference of young scientists and post-graduates. Uzhhorod, 21–24 May 2019. Proceedings of the conference. Uzhhorod, 2019, pp. 101–102.

[9] Pumplin, J. (1992), «Analysis of elastic scattering at low momentum transfer», Phys. Lett. B, V. 276, pp. 517–525.

[10] Desgrolard, P., Kontros, J., Lengyel, A.I., Martinov, E.S. (1997), «Local nuclear slope and curvature in high energy pp and $\overline{\text{pp}}$ elastic scattering», Nuovo Cim., V. 110A, pp. 615–630.

[11] Cohen-Tannoudji, G., Iljin, V. V., Jenkovszky, L. L., Tutik, R. S. (1972), «A model for the pomeron trajectory», Lett. Nuovo Cim., V. 5, pp. 957–962.

[12] Block, M., Cahn, B.N. (1985), «High-energy pp and forward elastic scattering and total cross sections», Rev. Mod. Phys. V.57, pp. 563–598.

[13] Dias de Deus, Jorge and Padua, Antonio Braz de(1993), «The search of asymptopia in soft physics at high energy», Phys. Lett. B, V. 317, pp. 428–432.

[14] Petrov, V.A., Okorokov, V.A. (2018), «The Size Seems to Matter or Where Lies the «Asymptopia»?», Int. J. Mod. Phys., V. A33, pp. 1850077.

[15] Schiz, A., Fajardo, L.A. *et al.* (1981), «High-statistics study of $\pi^+ p$, $\pi^- p$, and pp elastic scattering at 200 GeV/c», Phys. Rev. D, V. 24, pp. 26.

[16] Amaldi, U., Schubert, K.R. (1980), «Impact parameter interpretation of proton-proton scattering from a critical review of all ISR data», Nucl. Phys. B, V. 166, pp. 301–320.

[17] Bozzo, M., Braccini, P.L. *et al.* (UA4 Collaboration) (1985), «Elastic scattering at the CERN SPS Collider up to a four-momentum transfer of 1.55 GeV^2», Phys. Lett. B, V. 155, pp. 197 – 202.

Н. Бенце[1], А.В. Лендел[2], З.З. Торич[2]

[1]Ужгородский национальный университет, 88000, Ужгород, ул. Университетская, 14, Украина
[2]Институт электронной физики НАН Украины,88017, г. Ужгород, ул. Университетская, 21, Украина
e-mail: bencenorbert007@gmail.com

МОДЕЛИ ПОМЕРОНА ПРИ ЕНЕРГИЯХ БАК

Значения наклона *B(s,t)* и параметра кривизны *C(s,t)* рассчитаны в широком интервале энергий *s* и при малых *t* с учетом формы дифракционного конуса. Предсказано убывание абсолютного значения параметра кривизны *C(s,0)* в зависимости от *s* с сменой знака при асимптотически высоких энергиях.
Ключевые слова: упругое рассеяние, высокие энергии, померон, наклон, кривизна.

Н. Бенце[1], О.І. Лендєл[2], З.З. Торич[2]

[1]Ужгородський національний університет, 88000, Ужгород, вул. Університетська, 14, Україна
[2]Інститут електронної фізики, НАН України, 88000, Ужгород, вул. Університетська, 21, Україна
e-mail: bencenorbert007@gmail.com

МОДЕЛІ ПОМЕРОНА ПРИ ЕНЕРГІЯХ ВАК

Значення нахилу *B(s,t)* та параметра кривини *C(s,t)* розраховані в широкому інтервалі енергій *s* та при малих *t* з урахуванням форми дифракційного конусу. Передбачається, що абсолютні значення параметра кривини *C(s,0)* зменшуються залежно від *s* із зміною знаку при асимптотично високих енергіях.
Ключові слова: пружне розсіювання, високі енергії, померон, нахил, кривина.

СПИСОК ВИКОРИСТАНОЇ ЛІТЕРАТУРИ

[1] Antchev G. Evidence of non-exponential elastic proton-proton differential cross-section at low $|t|$ and $\sqrt{s} = 8$ TeV by TOTEM / G. Antchev, I. Aspell *et al.* (TOTEM Collaboration) // Nucl. Phys. B. – 2015. – V. 899. – P. 527–546.

[2] Antchev G. First determination of the ρ parameter at $\sqrt{s} = 13$ TeV – probing the existence of a colorless three-gluon bound state / G. Antchev, I. Aspell *et al.* (TOTEM Collaboration) // Eur. Phys. J. C. – 2017. – V. 79. – P. 785 (1–26).

[3] Jenkovszky L. Low-$|t|$ structures in elastic scattering at the LHC / L. Jenkovszky, A. Lengyel //Acta Phys. Pol. B. – 2015. – V. 46. – P. 863–877.

[4] Khose V.A. Elastic proton-proton scattering at 13 TeV / V.A.Khose, A.D. Martin, M.G. Ryskin // Phys. Rev. D. – 2018. – V. 97. – P. 034019.

[5] Martynov E. Did TOTEM experiment discover the Odderon? / E. Martynov, B. Nicolescu // Phys. Lett. B. – 2018. – V. 778. – P. 414–418.

[6] Antchev G. Measurement of Elastic pp Scattering at $\sqrt{s} = 8$ TeV in the Coulomb-Nuclear Interference Region - Determination of the ρ Parameter and the Total Cross-Section

/ G. Antchev, I. Aspell *et al.* (TOTEM Collaboration) // Eur. Phys. J. C. – 2016. – V. 76. – P. 661 (1–21).

[7] Desgrolard P. Nonlinearities and Pomeron nonfactorizability in convention diffraction / P. Desgrolard, A.I. Lengyel and E.S. Martinov // Nuovo Cimento. – 1997. – V. 110. – P. 251 – 266.

[8] Bence N. Comparative analysis of analytical models for high energy pp-scattering / N. Bence, A.I. Lengyel, Z.Z Tarics // IEP-2019. International Conference of young scientists and post-graduates. Uzhhorod, 21–24 May 2019. Proceedings of the conference. Uzhhorod, P. 101–102.

[9] Pumplin J. Analysis of elastic scattering at low momentum transfer / J. Pumplin // Phys. Lett. B. – 1992. – V. 276 – P. 517–525.

[10] Desgrolard P. Local nuclear slope and curvature in high energy pp and $\overline{\text{pp}}$ elastic scattering / P. Desgrolard, J. Kontros, A.I. Lengyel, E.S. Martinov // Nuovo Cim. – 1997. – V. 110A. – P. 615–630.

[11] Cohen-Tannoudji G. A model for the pomeron trajectory / G. Cohen-Tannoudji, V.V. Iljin, L.L. Jenkovszky, R.S. Tutik // Lett. Nuovo Cim. – 1972. – V. 5. – P. 957–962.

[12] Block M. High-energy pp and forward elastic scattering and total cross sections / M. Block, B.N. Cahn // Rev. Mod. Phys. – 1985. – V. 57. – P. 563–598.

[13] Dias de Deus Jorge The search of asymptopia in soft physics at high energy / Jorge Dias de Deus, Antonio Braz de Padua // Phys. Lett. B. – 1993. – V. 317. – P. 428–432.

[14] Petrov V.A. The Size Seems to Matter or Where Lies the «Asymptopia»? / V.A. Petrov, V.A. Okorokov // Int. J. Mod. Phys. – 2018. – V. A33. – P. 1850077.

[15] Schiz A. High-statistics study of $\pi^+ p$, $\pi^- p$, and pp elastic scattering at 200 GeV/c / A. Schiz, L.A. Fajardo *et al.* // Phys. Rev. D. – 1981. – V. 24. – P. 26.

[16] Amaldi U. Impact parameter interpretation of proton-proton scattering from a critical review of all ISR data / U. Amaldi, K.R. Schubert // Nucl. Phys. B. – 1980. – V. 166. – P. 301–320.

[17] Bozzo M. Elastic scattering at the CERN SPS Collider up to a four-momentum transfer of 1.55 GeV^2 / M. Bozzo, P.L. Braccini, *et al.* (UA4 Collaboration) // Phys.Lett. B. – 1985. – V. 155. – P. 197–202.